JOURNAL OF OPTOELECTRONICS AND ADVANCED MATERIALS Vol. 12, No. 2, February 2010, p. 212 – 218

Electrical and photoelectrical properties of organic photovoltaic cells based on polymer blends ITO/PEDOT/P3HT: PCBM (1:1)

L. MAGHERUSAN[a], P. SKRABA[b], C. BESLEAGA[a], S. IFTIMIE[a], N. DINA[a], M. BULGARIU[a], C.-G. BOSTAN[a], C. TAZLAOANU[a], A. RADU[a], L. ION[a], M. RADU[a], A. TANASE[a], G. BRATINA[b], S. ANTOHE[a,c*]
[a]*University of Bucharest, Faculty of Physics, 405 Atomistilor street, PO Box MG-11, 077125, Magurele, Ilfov, Romania*
[b]*University of Nova Gorica, Vipavska 13, POB SI-5000 Nova Gorica, Slovenia*
[c]*"Horia Hulubei"Foundation, Bucharest, Magurele – Ilfov, Romania*

Photovoltaic structures based on poly(3-hexylthiophene) (P3HT), 1-(3-methoxycarbonyl)-propyl-1-phenyl-(6,6)C_{61} (PCBM) polymers and P3HT:PCBM(1:1) polymers blend, respectively, were prepared by spin coating technique, using optical glass substrates covered with 30 nm thick ITO. The current-voltage (I-V) characteristics, in dark and illumination through ITO electrode of the ITO/PEDOT/P3HT/Al, ITO/PEDOT/PCBM/Al and ITO/PEDOT/P3HT: PCBM (1:1)/Al, structures were measured. Their non-linearity and asymmetry were explained on the base of electrode/organic semiconductor interface behavior. The measured action spectra of the cells revealed the features also observed in absorption spectra of the component polymers or the blend. A fill factor (FF) of 28%, higher than in the case of single layer structures was measured experimentally for the blend structures. The power conversion efficiency on 0.44%, of the as prepared blend structures was higher, too, than those of the single layer structures based on the ordinary P3HT and PCBM layer, respectively. The fourth quadrant parameters of the blend structures, determined in monochromatic light, change in time with respect of their values obtained on as prepared samples.

(Received February 8, 2010; accepted February 18, 2010)

Keywords: Polymer blends, P3HT, PCBM

1. Introduction

Since Tang [1] first presented a thin film organic solar cell based on a donor-acceptor heterojunction two decades ago, tremendous effort has been invested in improving the power conversion efficiency (η) of organic photovoltaic devices. The first organic photovoltaic cells were on Schottky type M1/ Organic layer/ M2 (M1 and M2 metals with different work function, in such a way that one contact should be ohmic and the other one a blocking contact). In these structures the organic dye was the monomeric phthalocyanines, merocyanines, porphiryns, e. a., and the photovoltaic response is due to the separation of the photogenerated charge carriers in the built electric

field present at the rectifying metal/semiconductor interface. The power conversion efficiency was small of the order of 10^{-2} % [2]. Using two-layered structures in which the photoactive region is the heterojunction between two organic layers, with complementary absorption spectra, the power conversion efficiency was increased with about two orders of degree [3], than in the case of single layer structures. Trying to enlarge the photoactive region three-layered structures were reported with an increased efficiency due to the number of sites for exciton dissociation [4]. Following the photovoltaic mechanism, an excitonic one, which takes place in this kind of cells, the structures based on polymeric blends, seem to be more promising for photovoltaic cells with relatively high efficiency about 4-5%, but more cheap than the organic monomeric thin films [5]. Among the large range of polymeric materials tested as active layers, polymer-fullerene bulk heterojunction solar cells have shown promising perspectives because of the high quality of these materials in terms of mobility and thermal stability [6-10]. Here we present structural, morphological, electrical and photoelectrical properties of organic photovoltaic cell based on poly (3-hexyltiophene) (P3HT), 1-(3-methoxycarbonyl)-propyl-1-phenyl-(6, 6) C61 (PCBM). We stress the differences observed for the devices based on single components and those fabricated from blend of the above polymers.

2. Experimental procedures

The anode has been patterned on ITO-coated glass, commercially available from Praezisions Glass und Optik (CECO20P). The cleaning of the substrates, prior to the deposition of the active layers, consisted in ultrasonication in acetone and rising in isopropanol and deionized water. Deposition of a commercially available poly (ethylenedioxythiophene): polystyrene sulfonic (PEDOT-PSS) acid layer (100 nm thick) by spin coating was done on ITO-coated glass, during 60s at the angular velocity of 6000rot/s, the acceleration needing to reach this speed being 10000rot/s^2. This layer is used to facilitate the hole transfer between the active layer and the ITO electrode, due, one a hand, to its ability to help smooth both the surface roughness and the conductivities of commercial ITO glass substrate, and the other hand, due to the fact that its work function lies between the work function of ITO

(4.7 eV) and the HOMO levels of most p-type organic semiconductors. Regio-regular P3HT and PCBM were purchased from Aldrich and used as received. All the polymeric films (P3HT, PCBM and P3HT: PCBM, 1:1 blend, respectively) were deposited on PEDOT layer, by spin coating in two steps: the first during 70s with an angular velocity of 1500rot/s and acceleration of 1000rot/s^2 and second step in 20s with an angular velocity of 2000rot/s and the same acceleration. An Al top contact was deposited by vacuum thermal evaporation to complete the photovoltaic structures. The residual pressure in the chamber was 10^{-5} Torr and the samples were maintained at room temperature during deposition. A cross section through the prepared samples is shown in Fig. 1.

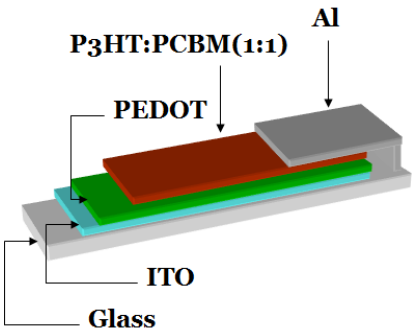

Fig.1. Structure of the photovoltaic cells based on P3HT, PCBM or P3HT: PCBM blend, respectively

Absorption spectra were recorded at room temperature using a UV-VIS Perkin-Elmer Lambda 35 Spectrophotometer. Action spectra were performed with a set-up consisting of a Cornerstone 130 monochromator and a Keithley 2400 Source Meter, controlled by a computer. The current-voltage (I-V) characteristics of the cells, both in dark and under illumination with monochromatic light, at wavelength corresponding to the maximum in action spectrum for each sample, were measured at room temperature. Moreover, the fourth quadrant I-V characteristics were recorded under monochromatic light with different wavelength in action spectrum of each investigated structure. The morpho-structural features of the samples were evidenced by Atomic Force Microscopy using an Ape Research SPM (AFM A100-SGS) apparatus. The roughness and thickness of the thin films was determined by X-ray reflectometry using a Bruker D8 Discover XRD difractometer.

3. Results and discussion

3.1 Morphological Investigations

X-ray reflectivity is sensitive to thin films having the thickness in the range of atomic dimensions to many tens of microns, by virtue of the X-ray wavelengths employed and the very high diffraction space resolutions attainable.

The strong interference between the different boundaries index give rise to fringing from which the thickness can be estimated using $t = \frac{(i-j)\lambda}{2\sin(\omega_i - \omega_j)}$, where i and j are the fringe orders and ω_i' , ω_j' their corresponding half of the scattering angles, respectively. This is simply derived from Bragg's law and was first used for thickness determination with reflectometry by Keissing [11]. The reflectometry curves recorded for the ITO/PEDOT/P3HT/Al, ITO/PEDOT/PCBM/Al and ITO/PEDOT/P3HT: PCBM (1:1)/Al cell with the Cu $k_{\alpha\,1}$ line, λ = 1.5406 A, are shown in figure 2, figure 3 and Fig. 4, respectively.

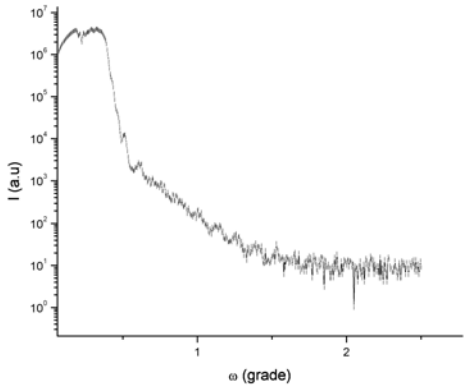

Fig.2. Reflectometry curve for ITO/PEDOT/P3HT film.

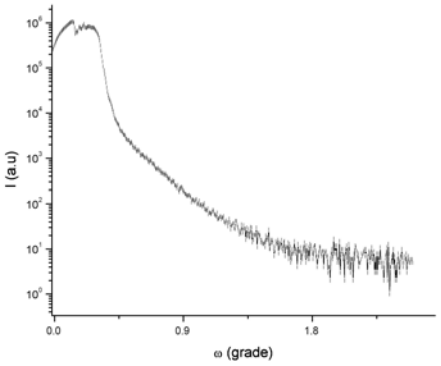

Fig. 3. Reflectometry curve for ITO/PEDOT/PCBM film.

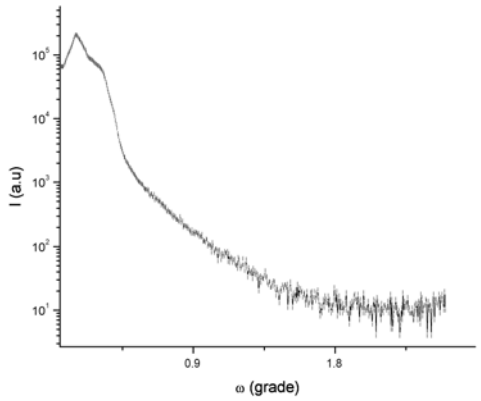

Fig. 4. Reflectometry curve for ITO/PEDOT/P3HT: PCBM (1:1) film.

The thickness and roughness values had been calculated for the films from the experimental curves using the LEPTOS software package. The obtained values are shown in Table 1.

Table 1. The thickness and roughness values for the ITO/PEDOT/P3HT, ITO/PEDOT/PCBM and ITO/PEDOT/P3HT: PCBM (1:1)

Sample	Thickness(nm)	Roughness(nm)
S1	97	10
S2	139	15
S3	123	13

S1: ITO/PEDOT/P3HT film
S2: ITO/PEDOT/PCBM film
S3: ITO/PEDOT/P3HT: PCBM (1:1) film

One can notice in Table 1 that the prepared structures exhibited low values of roughness and thickness. Such values of roughness are typical for spin coating polymeric films. It is known that a reduced thickness of the films should lead to reduced compressive stresses, conferring to the structure a good mechanical integrity.

3.2 Electrical and photoelectrical experimental results for the ITO/PEDOT/P3HT/Al cells

The measured current-voltage characteristics in the dark through ITO electrode of ITO/PEDOT/P3HT/Al cell, after 2h Al top contact deposition are shown in figure 5.

The dark I-V characteristic of ITO/PEDOT/P3HT/Al cell was measured at room temperature, and in both forward and reverse bias condition. The forward bias conditions correspond to positive voltage on the ITO electrode with respect to the Al top contact electrode.

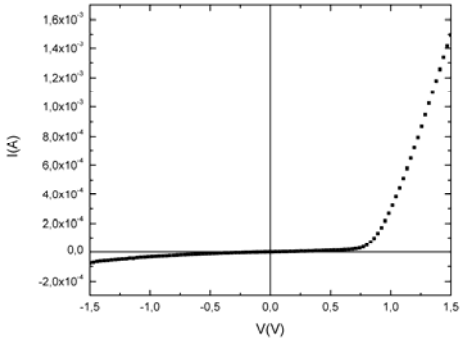

Fig. 5. I-V characteristics of ITO/PEDOT/P3HT/Al cell in the dark..

As seen, in figure 5, the I-V dependence is non-linear and highly asymmetric, with a rectifying factor ($R_R=I_f/I_r$ at the same voltage V), of about 200 at 1.5 V, but increasing up to 500 at the 3.5 V, maximum value of forward applied voltage. Taking into account that P3HT is an electron donor (hole acceptor) with the orbital levels shown in figure 6 and Al is a small work function electrode (SWFE) [12], we suppose that this asymmetry is due to the presence of a blocking contact (Schottky barrier) at the Al/P3HT interface, while the interface ITO/PEDOT/P3HT behaves about like an ohmic contact, talking on holes like the majority charge carriers.

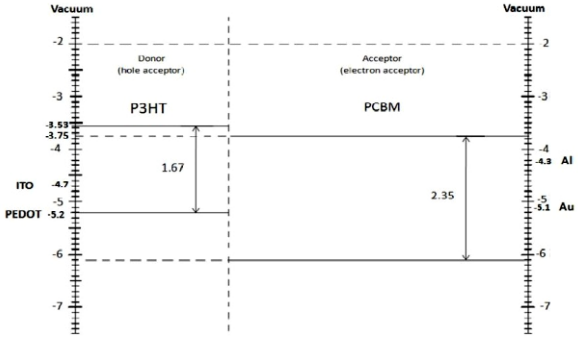

Fig. 6. Orbital levels of P3HT and PCBM together with work functions of ITO, PEDOT, Al and Au

A thorough analysis of the dark I-V characteristic of the cell, starting from the modified Shockley equation, valid for Schottky barrier too [4], allow to have a good characterization of Al/P3HT interface, responsible for both electric and photovoltaic behavior of the cell.

The modified Shockley equation is given by:

$$I = I_0[\exp[\beta(V - R_s I)] - 1] + (V - \eta_2 I)/R_{sh} \quad (1)$$

where: I_0 is the reverse saturation current, R_s – the series resistance and R_{sh} – the shunt resistance. Here $\beta = q/nkT$, where: q is the electronic charge, n – the diode quality factor, k – the Boltzmann constant, and T – the absolute temperature. The differential resistance of the cell is given by:

$$R_D = R_s + 1/[\beta I_0[\exp[\beta(V - \eta_2 I)] + \frac{1}{R_{sh}}] \quad (2)$$

At high voltages, in forward bias, Eq. (1) becomes $I = I_0 \exp[\beta(V - \eta_2 I)]$ and then Eq. (2) simplifies to:

$$R_D = R_s + 1/(\beta I) \quad (3)$$

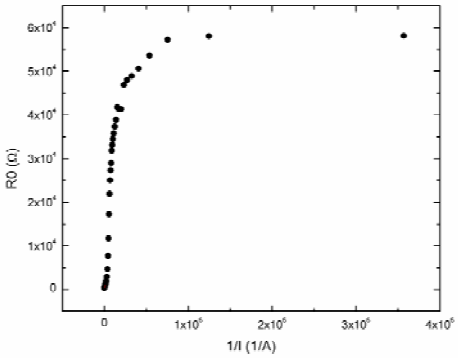

Fig. 7. Dependence of the differential resistance of ITO/PEDOT/P3HT/Al cell on the reciprocal of the current at forward bias

Thus, from the range of high voltages of R_0 vs. 1/I plot, shown in figure 7, the values for R_s and n parameters can be extracted. At low voltages, where the current flowing through R_{sh} becomes important, Eq. (2) becomes $R_0 = R_s + R_{sh}$. Since $R_s \ll R_{sh}$, it follows that R_0 is essentially R_{sh} at low voltages. The values of R_s and R_{sh} are: $R_s = 328\ \Omega$ and $R_{sh} = 58.13\ K\Omega$.

Further on, in order to get with more accuracy the values of I_0 and n, Eq. (1) has been transformed

$$\text{as: } I - \frac{Y}{R_{sh}} = I_0[\exp(\beta Y)] \qquad (4)$$

where: $I - \frac{Y}{R_{sh}}$ is the current flowing through the barrier and $Y = V - R_s I$, the really drop voltage just across it, respectively.

The plot of $\ln(I - Y/R_{sh})$ vs. Y is shown in figure 8. We can see that removing the effects of series and shunt resistance, the linear part in the obviously $\ln I = f(V)$ plot was extending, increasing the accuracy in the calculus of I_0 and n. The values I_0 and n obtained from the fit of our experimental data with the Eq. (4) are $I_0 = 7.2\times10^{-11}$ A and $n = 2.29$, respectively.

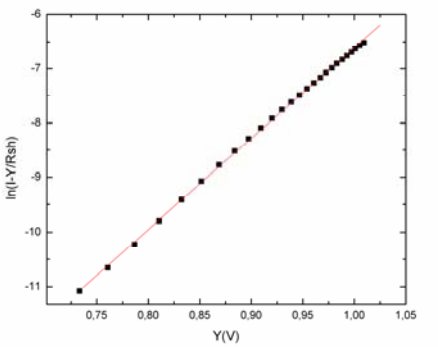

Fig.8. The ln(I-Y/R_{sh}) = f(Y) characteristics for ITO/PEDOT/P3HT/Al cells.

The absorption spectrum of P3HT layer together with the action spectrum of the short-circuit photocurrent of the ITO/PEDOT/P3HT/Al cell are shown in Fig. 9.

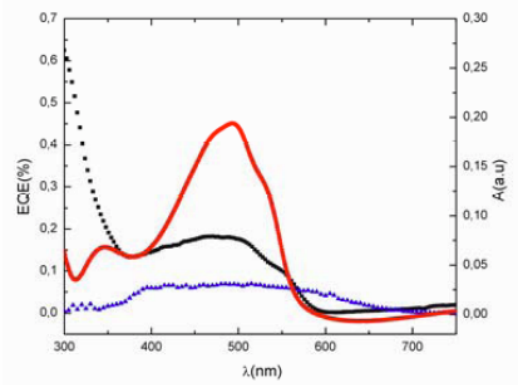

Fig. 9. The action spectra normalized to the power of the light source of the ITO/PEDOT/P3HT/Al cell, after 2h (black curve), and 48h (blue curve) Al top contact deposition, respectively. The red line represents the absorption spectrum of P3HT thin film.

Both spectra were obtained under illumination through ITO electrode and they seem to be batic spectra, with a small shift towards shorter wavelengths. These batic spectra could be explained such as follows. At illumination through ITO electrode the photovoltaic response is given by the separation of the photo generated charge carriers resulting from the excitons dissociation in the internal electric field present at the Al/P3HT interface, which seem to be extended in the whole volume of P3HT layer with small thickness (Table 1), and then the hole dominant component of photocurrent, follows the absorption spectrum of P3HT. Nevertheless, the maximum of the action spectrum, located at 471 nm, is shifted towards shorter wavelengths as compared to the maximum appearing at 497 nm in the absorption spectrum. A possible explanation is that at shorter wavelengths carriers' photo generation is stronger near the PEDOT surface rather than deep in the bulk of the P3HT layer. Due to the inherent presence of defect states at the PEDOT/P3HT interface, this could lead to the recombination of the photo generated carriers. Also at wavelengths shorter than 400 nm, incident photons are highly absorbed in the ITO/PEDOT electrode itself, through fundamental absorption mechanism, and the photovoltaic effect at ITO/PEDOT/P3HT junction is suppressed.

3.3 Experimental results for the ITO/PEDOT/PCBM/Al cells

The dark I-V characteristics, at room temperature, for both forward and reverse bias, obtained for this sample are shown in Fig. 10. The forward bias conditions correspond to positive voltage on the ITO contact with respect to the other one (Al electrode).

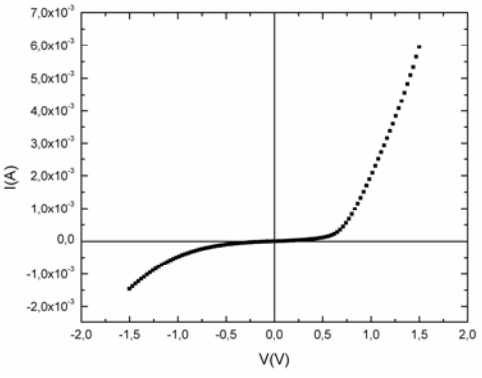

Fig. 10. The dark I-V characteristics of ITO/PEDOT/PCBM/Al cells

The I-V dependence is asymmetric, with a rectifying factor R_R of about 10 at 2 V. Now, taking into account that PCBM is an electron acceptor (n-type semiconductors) with the orbital levels shown in figure 6 and Al is a small work function electrode [12], we suppose that this asymmetry is due to the presence of a blocking contact at the ITO/PEDOT/PCBM interface, while the interface Al/PCBM behaves like an ohmic contact, talking on the

electrons like majority charge carriers in PCBM. The values of R_s, R_{sh}, n, I_0, obtained by the method previously presented are: $R_s=113\ \Omega$, $R_{sh}=9730\ \Omega$, $n=2.8$, $I_0=4\times10^{-8}\ A$.

The optical absorption spectrum of PCBM film and the action-spectrum of I_{sc} of a typical ITO/PEDOT/PCBM/Al cell are plotted in figure 11. Both spectra were obtained under illumination through ITO electrode. One can easily notice the anti-batic response of the PCBM layer, was obtained, i.e., maximum photocurrent is obtained for photon energies where the absorption is about at its minimum. This is due to the filtering effect of the PCBM film. The photons strongly absorbed in PCBM give rise to the dissociation of the excitons, and then to the photo charge carriers, far away from the ITO/PEDOT/PCBM interface (photoactive region). More that being a relatively thick layer the photo generated electrons, the majority charge carriers, strongly recombine before to reach the Al electrode.

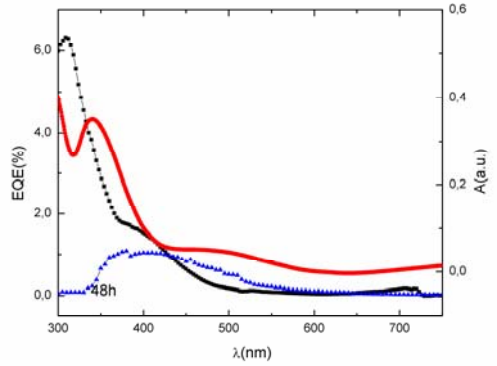

Fig. 11. Photocurrent normalized to the power of the light source: 2h (black curve), and respectively 48h (blue curve) after the Al deposition and the corresponding absorption spectrum of PCBM (red curve) for the ITO/PEDOT/PCBM/Al structure.

3.4 Experimental results for the ITO/PEDOT/P3HT:PCBM(1:1)/Al cells

Fig. 12 shows the I-V characteristic of a typical ITO/PEDOT/P3HT: PCBM (1:1)/Al cell in the dark, at room temperature, for both forward and reverse bias.

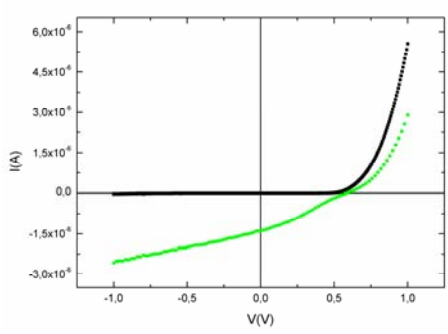

Fig. 12. I-V characteristics of ITO/PEDOT/P3HT: PCBM (1:1)/Al at dark (black curve) and under 400 nm monochromatic light (green curve).

The forward conditions correspond to positive voltage on the ITO electrode with respect to the other Al one. As seen in figure 11, the I-V dependence is non linear and highly asymmetric, with a rectifying factor of about 120 at 1 V, increasing when applied voltage increases. Knowing the behavior of the sample ITO/PEDOT/P3HT/Al and ITO/PEDOT/PCBM/Al, above described, we suppose that this asymmetry is due to the difference between work function of ITO/PEDOT and Al electrode, respectively, the Al/P3HT: PCBM (1:1) blend interface being a good electron collector since the ITO/PEDOT/P3HT: PCBM (1:1) blend interface behave like a good holes collector.

The action spectra of ITO/PEDOT/P3HT: PCBM (1:1)/Al cells together with absorption spectrum of the P3HT: PCBM (1:1) blend layer, under illumination through ITO electrode, are shown in figure 13. The photovoltaic properties for the blend cells are by far better than those observed for single-layer cells, based on P3HT and PCBM layer, respectively.

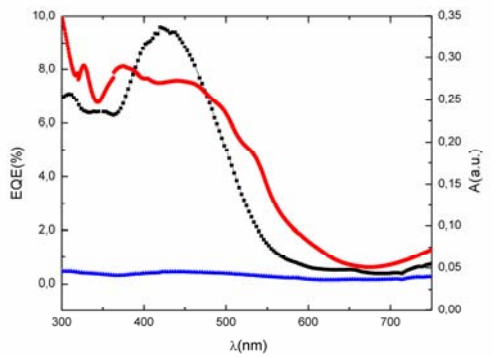

Fig. 13. Photocurrent normalized to the power of the light source: 2h (black curve), and respectively 48h (blue curve) after the Al deposition for the ITO/PEDOT/P3HT: PCBM (1:1)/Al structure and the corresponding absorption spectrum of the P3HT: PCBM (1:1) blend (red curve).

The blend cell shows an improved (wider) spectral response as compared to the case of single layer cells. The absorption spectrum of the blend P3HT: PCBM (1:1) was enlarged from 300 nm until 700 nm, containing the mainly range of P3HT spectrum (400 nm – 700 nm) and that of PCBM spectrum (300 nm – 500 nm), showing that the so call "Co sensitization effect" still exist in the case of blend structures like in the case of D/A bilayer cell [13, 14]. The action spectra are enlarged too, in the range (300 nm – 600 nm) with increased photocurrent, as compared to the case of single layer cells. The maximum in the action spectrum (at 430 nm) is slightly red-shifted as compared to the local maximum at 380 nm in the optical absorption, having the tendency to follows the action spectra of the ITO/PEDOT/P3HT/Al cell than that of ITO/PEDOT/PCBM/Al structures.

As expected in the case of the blend structures, the number of Donor/Acceptor (D/A) interfaces was significantly increased by blending the two donor and acceptor materials, giving rise to the so call "bulk

heterojunction", in which the dimension of photon-capturing domain becomes on the same order of average exciton diffusion lengths, which is between 5 and 50 nm for most organic semiconductors. In this case the larger D/A interface reduces the exciton loss, one a hand, and on the other hand, the thicker blend film harvest more photons reducing then the photon loss in than case of single P3HT or PCBM layer cells.

However, even though a stronger photo generation takes place in a blend, the carrier loss seem to be a major problem, due to the fact that the charge carriers can be easily trapped in the isolated phase donor or acceptor domains which still coexist with the blend. More that, if the donor and acceptor are in direct contact with both collector electrodes, the recombination of the non-equilibrium charge carriers at the blend/electrodes interface could be strong enough. As we can see in figure 13, the action spectra of blend structure, has an anti-batic behavior. Even though the energy offsets between Donor – LUMO and Acceptor – LUMO represent the key driving force for the exciton dissociation, then for the enhanced photocurrent in a blend structure [15], the presence of the internal electric field across the electrodes, has an important contribution to the photovoltaic response, too [16]. In these terms we try to explain the measured anti-batic spectra presented in figure 13. Observing, the tendency of the action spectra of the blend structures to follows the action spectra of the ITO/PEDOT/P3HT/Al cell, we suppose that the internal electric field across the Blend/Al interface has an important contribution to photocurrent, by its hole components. The illumination taking place through ITO electrode and the thickness of the blend film is large (see table 1), we suppose that the filtering effect is present here. Namely, the maximum photocurrent is obtained for photon energies where the absorption in the blend, is at its minimum. The photons strongly absorbed in P3HT: PCBM (1:1) blend give rise to charge carriers far away from the P3HT: PCBM (1:1)/Al interface. The photons slighter absorbed in the volume of the blend layer will generate photo charge carriers in the region of this internal electric field then participating to the photovoltaic response too, even though the energy offsets between donor and acceptor remain the mainly driving force for the exciton dissociation.

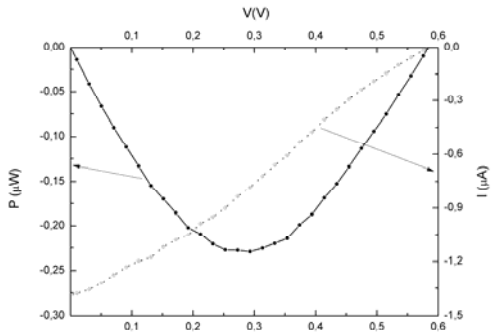

Fig. 14. The fourth quadrant I-V characteristic of the ITO/P3HT: PCBM (1:1)/Al device under illumination with 400 nm monochromatic light and P_{in}= 5.19×10^{-5} W.

The fourth quadrant of I-V characteristics of ITO/PEDOT/P3HT: PCBM (1:1)/Al cell measured at illumination under 400 nm monochromatic light (green curve in figure 11), is shown in figure 14.

The measured values of these parameters, see Table 2, (even though modest) show an important improvement of photovoltaic behavior of the blend P3HT: PCBM (1:1) based structures as compared with the single polymer P3HT or PCBM based structures.

Table 2. The typical parameters in regime on photo element: Open-circuit photo voltage (V_{0C}), Short-circuit photocurrent (I_{ph}), Maximum output power (P_m), Incident light power (P_{in}), Fill factor (FF), Power conversion efficiency (η) of: ITO/PEDOT/P3HT/Al, ITO/PEDOT/PCBM/Al and ITO/PEDOT/P3HT: PCBM (1:1)/Al structures.

Parameter	S1	S2	S3
V_{OC} (V)	0.84	0.1	0.58
I_{ph} (A)	1.85x10^{-8}	4.1x10^{-8}	1.35x10^{-6}
P_m (W)	1.7x10^{-9}	5.88x10^{-10}	2.25x10^{-5}
P_{in} (W)	2.15x10^{-5}	3.3x10^{-5}	5.19x10^{-5}
FF (%)	10	14	28
η (%)	0.01	0.0017	0.44

S1: ITO/PEDOT/P3HT/Al cells
S2: ITO/PEDOT/PCBM/Al cells
S3: ITO/PEDOT/P3HT: PCBM (1:1)/Al cells

What is typical features for these kinds of structures is the fact that their stability in time is very poor. In our study such as you can see in figures 9, 11 and 13, we measured the action spectra after 2 hours from the Al contact deposition and after 48 hours after its deposition, too, observing permanently the decreasing of the photocurrent in this so short time.

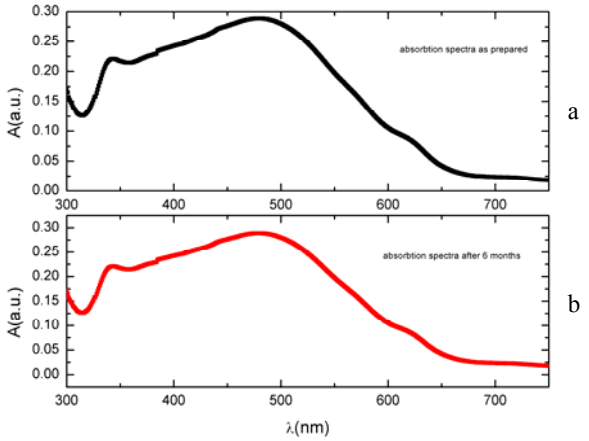

Fig. 15. Absorption spectra of the blend P3HT: PCBM (1:1) layer as prepared (a) and after 6 months (b).

Above, when we explain the electrical and photoelectrical behavior of each structure, we referred to the action spectra measured after 2h (considered as

prepared). Trying to explain this behavior we measured the absorption spectra for all the polymeric layers (P3HT, PCBM and P3HT: PCBM (1:1), respectively) deposited by spin coating, in the same conditions like those of investigated structures, to have the same structure and morphology, at different intervals of time. In the figure 15 the absorption spectra of the blend P3HT: PCBM (1:1) layer as prepared (black line) and after 6 months (red line) are shown as example. Such we can see, do not appear changes between them, in this long time, resulting that no changes take place in the optical processes giving rise to the excitons creation in these materials. But there are dramatically changes in physical processes involved in the photo generation of the charge carriers, their separation and collection to the electrodes. Now, systematically studies are carried out, devoted to explain these processes in view to the increasing the stability of the promising photovoltaic structures.

4. Conclusions

Polymer (P3HT, PCBM and their blend) based photovoltaic cells were produced by spin coating technique. I-V characteristics were measured in dark and under monochromatic light conditions. The parameters characterizing the region of internal electric field responsible both for the electrical behavior and photovoltaic response of the investigated structures were determined. The sample containing P3HT only as active layer shows a photovoltaic response due to the exciton dissociation in the internal electric field present at Al/P3HT interface. Al/PEDOT/PCBM/ITO sample shows a very low photovoltaic response, acting almost as a simply photo resistance.

The structures based on the P3HT: PCBM (1:1) blend shows a promising photovoltaic response, with a value of 0.58 V for the open-circuit voltage, and a short-circuit current of 1.35×10^{-6} A, increased of about two order of degree, than that measured in the case of structures based on P3HT or PCBM polymers. The measured fill factor and power conversion efficiency in the case of the blend structures were significantly increased as compare with their values measured in the case of structures based on P3HT or PCBM polymers. The P3HT: PCBM (1:1) blend is a very promising material for polymeric photovoltaic cells but optimizations studies in both spatial and energy/time domains should be performed to increase their power conversion efficiency.

Acknowledgements

This work was supported by National Authority for Scientific Research under Bilateral Cooperation No. 5CB/2008.

References

[1] C. W. Tang, Appl. Phys. Lett., **48**, 183 (1986)
[2] S. Antohe, Phys.Stat.Sol.(a),136, 401 (1993).
[3] S. Antohe, L. Tugulea, Phys.Stat.Sol. (a), **128**, 253 (1991)
[4] S. Antohe, V. Ruxandra, L. Tugulea, V.Gheorghe, D. Inascu, J. Phys. III France **6**, 1133 (1996).
[5] L. Schmidt-Mende, A. Fechtenkötter, K. Müllen, E. Moons, R.H. Friend, J. D. MacKenzie, Science **293**, 1119 (2001).
[6] Padinger, F.; Rittberger, R. S.; Sariciftci, N. S. Adv. Funct. Mater. **13**, 85 (2003).
[7] D. Chirvase, J. Parisi, J. C. Hummelen, V. Dyakonov, Nanotechnology **15**, 1317 (2004).
[8] G. Li, V. Shrotriya, Y. Yao, Y. Yang, J. Appl. Phys. **98**, 043704 (2005).
[9] P. Schilinsky, U. Asawapirom, U. Scherf, M. Biele, C. Brabec, J. Chem. Mater. **17**, 2175 (2005).
[10] Y. Kim, S. A. Choulis, J. Nelson, D. D. C.Bradley, S. Cook, J. R. Durrant, Appl. Phys. Lett. **86**, 063502. (2005)
[11] H. Keissing, Ann. Phys., Lpz. **10**, 769 (1931).
[12] Sam-Shajing Sun, Cheng Zhang, Chapter 14 pg.408 in Introduction to Organic Electronic and Optoelectronic materials and Devices, Edited by Sam-Shajing Sun, Larry R. Dalton, CRC Press, Taylor and Francis Group.
[13] M. Hiramoto, H. Fujiwara, M. Yokoyama, Appl.Phys. Let. **58**, 1062 (1991).
[14] S. Antohe, Chapter 11 ,,Electronic and Optoelectronic Devices Based on Organic Thin Films ‘’ in HANDBOOK OF ORGANIC ELECTRONICS AND PHOTONICS, Electronic Materials and Devices, Edited by Hari Singh Nalwa, Volume 1: Pages: 433, 440, AMERICAN SCIENTIFIC PUBLISHERS, Los Angeles, California, USA, 2006, ISBN : 1-58883-096-9.
[15] S. Sun,d N. S. Sariciftci (eds), Organic Photovoltaics: Mechanisms, Materials and Devices, CRC Press, Boca Raton, FL, 2005
[16] B. A. Gregg, Coulomb forces in excitonic solar cells, in S. Sun and N. S. Sariciftci (eds), Organic Photovoltaics: Mechanisms, Materials and Devices, CRC Press, Boca Raton, FL, 2005, p.139

*Corresponding author: s_antohe@solidphysica.unibuc.ro